Snapshot Hyperspectral Imaging Based on Weighted High-order Singular Value Regularization

Niankai Cheng[1], Hua Huang[2], Lei Zhang[1], and Lizhi Wang[1]

[1]School of Computer Science and Technology, Beijing Institute of Technology, Beijing, China

[2]School of Artificial Intelligence, Beijing Normal University, Beijing, China

Snapshot Hyperspectral Imaging

Core Problem

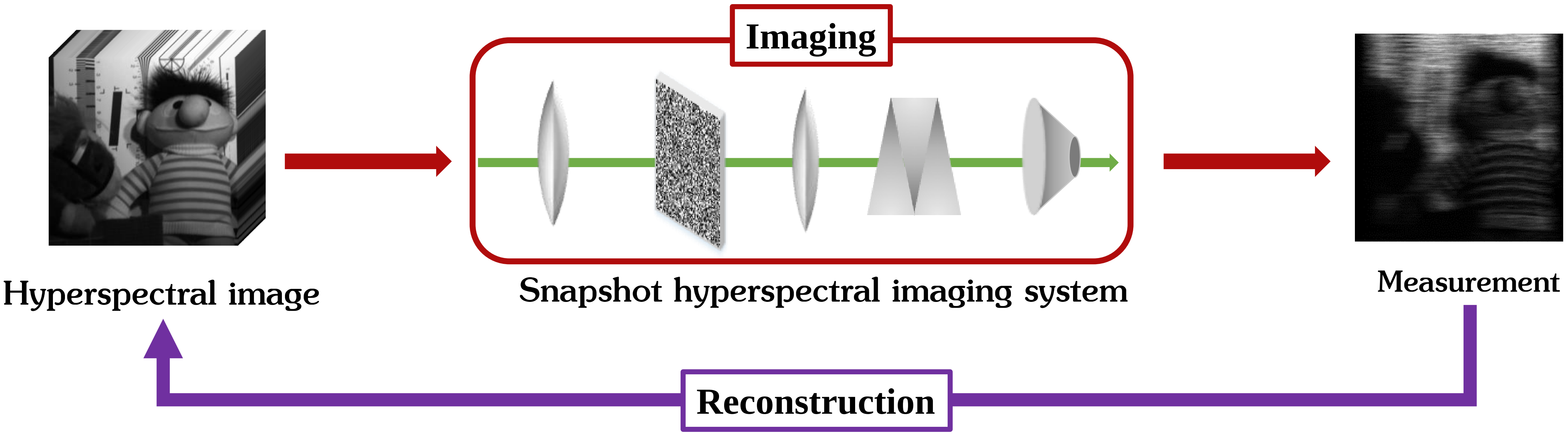

Problem formulation: $$\hat{\boldsymbol{\mathcal{F}}} = \min_{\boldsymbol{\mathcal{F}}} \underbrace{\boxed{\frac{1}{2}\|\boldsymbol{Y} - \boldsymbol{\Phi}(\boldsymbol{\mathcal{F}})\|_F^2}}_{\text{Data fidelity}} + \underbrace{\boxed{\tau\Gamma(\boldsymbol{\mathcal{F}})}}_{\text{Regularization}}$$

Related Work

Model Based Reconstruction

- ✓ Exploit the piecewise smooth property with total variation regularization, e.g., TV[1].
- ✓ Exploit spatial-spectral correlation via sparse representation, e.g., AMP[2], 3DSR[3], ANSR[4].
- ✓ Exploit spatial-spectral correlation via rank minimization, e.g., LRMA[5].

Learning Based Reconstruction

- ✓ Brute-force mapping from the compressive measurement, e.g., HSCNN[6].
- ✓ Exploit the non-linear sparsity via neuron shrinkage, e.g., AE[7], HRNet[8].
- ✓ Deep un-rolling with non-linear prior, e.g., ISTA-Net[9], SPR[10].

Motivation

Key Observation

- ✓ The vectorization process ignores the high-dimensionality nature of hyperspectral image and breaks the original structure.
- ✓ High-order tensors can provide a more accurate representation to figure out the data diversity in each domain and deliver the intrinsic structure of high-dimensionality signals.

Weighted High-order Singular Value Regularization

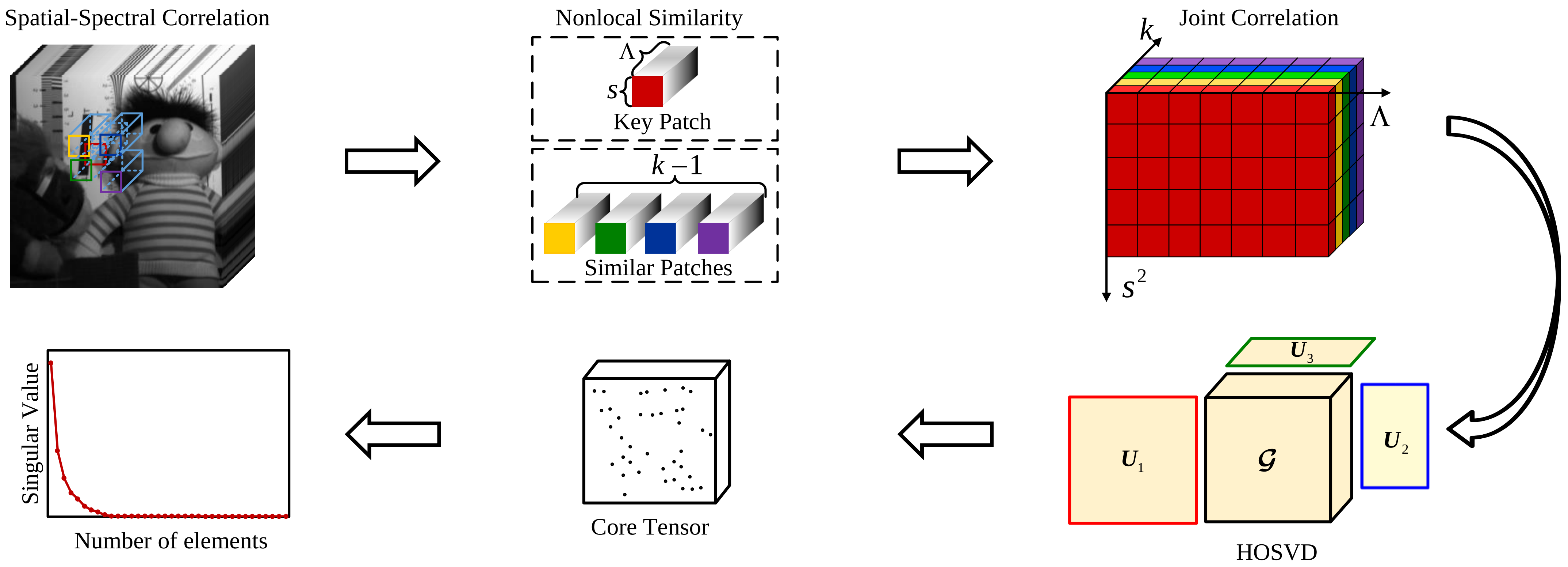

Weighted High-order Singular Value Regularization

Formulation: $$\Gamma(\mathcal{G}) = \tau \|\mathbf{R}(\mathcal{F}) - \mathcal{G} \times_1 \boldsymbol{U}_1 \times_2 \boldsymbol{U}_2 \times_3 \boldsymbol{U}_3\|_F^2 + \|\mathbf{w} \circ \mathcal{G}\|_1$$

Adaptive weights: $$\|\mathbf{w} \circ \mathcal{G}\|_1 = \sum_n w_n |g_n|, \quad w_n^{t+1} = c/\left(\left|w_i^t\right| + \varepsilon\right)$$

Reconstruction Algorithm

Reconstruction Problem

Formulation: $\min_{\mathcal{F},\mathcal{G}_l} \frac{1}{2}\|\boldsymbol{Y}-\boldsymbol{\Phi}(\mathcal{F})\|_F^2+\sum_{l=1}^{L}\left(\tau\|\mathbf{R}_l(\mathcal{F})-\mathcal{G}_l\times_1 \boldsymbol{U}_{l,1}\times_2 \boldsymbol{U}_{l,2}\times_3 \boldsymbol{U}_{l,3}\|_F^2+\|\mathbf{w}_l\circ\mathcal{G}_l\|_1\right)$

Updating Low-rank Tensors

Problem: $\min_{\mathcal{G}_l} \tau\|\mathbf{R}_l(\mathcal{F})-\mathcal{G}_l\times_1 \boldsymbol{U}_{l,1}\times_2 \boldsymbol{U}_{l,2}\times_3 \boldsymbol{U}_{l,3}\|_F^2+\|\mathbf{w}_l\circ\mathcal{G}_l\|_1$

Solution: $g_n=\max(\hat{g_n}-\frac{w_n}{2\tau},0)$

Updating the Whole Image

Problem: $\min_{\mathcal{F}} \frac{1}{2}\|\boldsymbol{Y}-\boldsymbol{\Phi}(\mathcal{F})\|_F^2+\sum_{l=1}^{L}\tau\|\mathbf{R}_l(\mathcal{F})-\mathcal{G}_l\times_1\boldsymbol{U}_{l,1}\times_2\boldsymbol{U}_{l,2}\times_3\boldsymbol{U}_{l,3}\|_F^2$

Solution: $\mathcal{F}=\left(\boldsymbol{\Phi}^T\boldsymbol{\Phi}+2\tau\sum_l\mathbf{R}_l^T\mathbf{R}_l\right)^{-1}\left(\boldsymbol{\Phi}^T(\boldsymbol{Y})+2\tau\sum_{l=1}^{L}\mathbf{R}_l^T(\mathcal{G}_l\times_1\boldsymbol{U}_{l,1}\times_2\boldsymbol{U}_{l,2}\times_3\boldsymbol{U}_{l,3})\right)$

Experiments

Performance on CASSI

Indexes	TV	AMP	3DSR	NSR	LRMA	AE	ISTA	HSCNN	HRecNet	SPR	Ours
PSNR	23.16	23.18	23.636	26.13	25.94	25.72	20.60	25.09	22.83	24.48	**28.05**
SSIM	0.7130	0.6600	0.7311	0.7610	0.7930	0.7720	0.5499	0.7334	0.6648	0.7395	**0.8302**
ERGAS	258.32	256.76	245.15	189.19	195.63	197.32	344.57	206.97	268.65	224.19	**153.06**
RMSE	0.0469	0.0474	0.0457	0.0333	0.0315	0.0333	0.0653	0.0373	0.0496	0.0451	**0.0236**

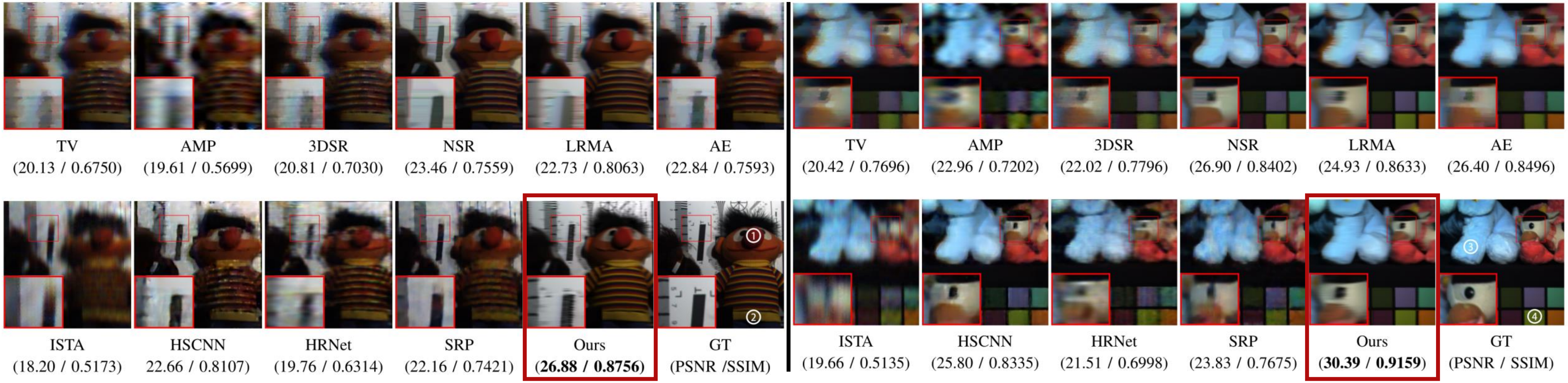

Experiments

Performance on DCCHI

Indexes	TV	AMP	3DSR	ANSR	LRMA	Ours
PSNR	23.16	23.18	23.636	26.13	25.94	**28.46**
SSIM	0.7130	0.6600	0.7311	0.7610	0.7930	**0.8277**
ERGAS	258.32	256.76	245.153	189.19	195.63	**147.84**
RMSE	0.0469	0.0474	0.0457	0.0333	0.0315	**0.0240**

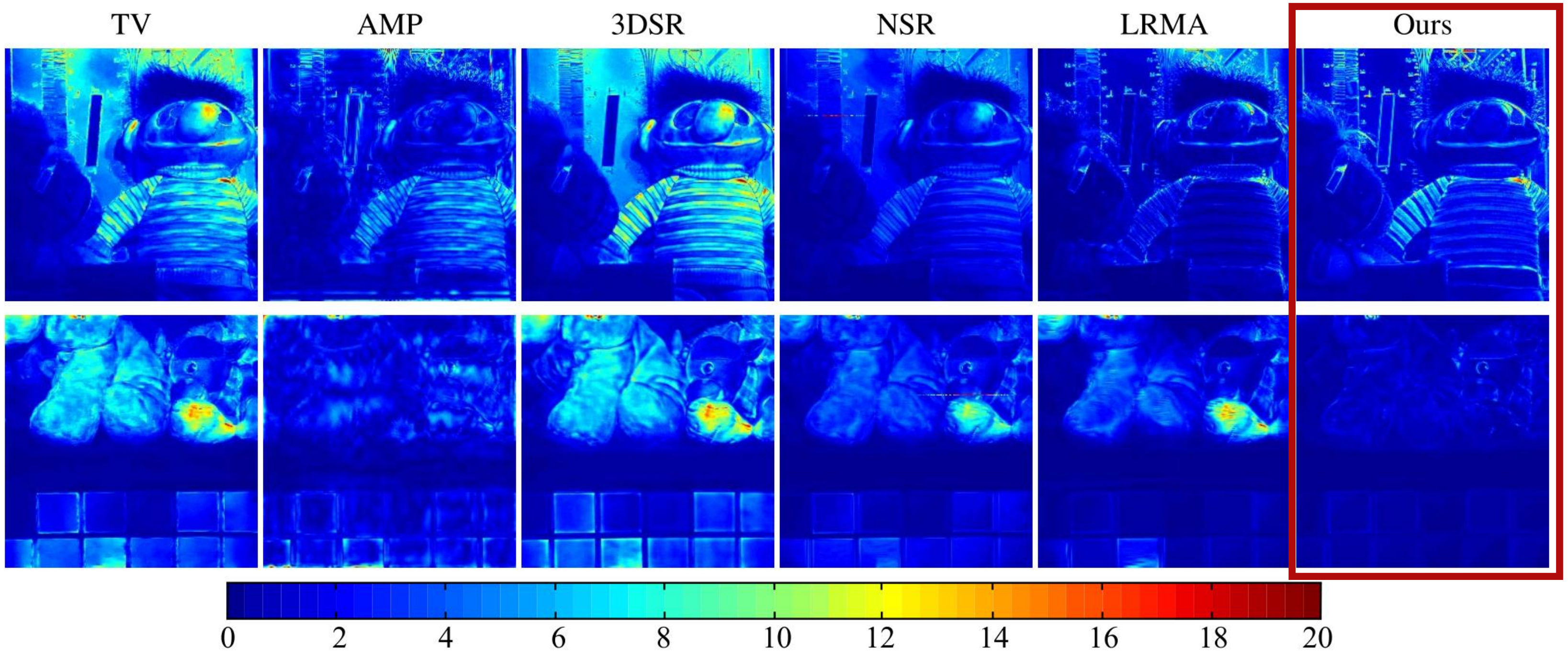

Reference

[1] Wagadarikar A, et al. Spectral image estimation for coded aperture snapshot spectral imagers. Image Reconstruction from Incomplete Data V. International Society for Optics and Photonics, 2008, 7076: 707602.
[2] Jin Tan, et al. Compressive hyperspectral imaging via approximate message passing. IEEE Journal of Selected Topics in Signal Processing, 2015, 10(2): 389-401.
[3] Xin Lin, et al. Spatial-spectral encoded compressive hyperspectral imaging. ACM Transactions on Graphics, 2014, 33(6): 1-11.
[4] Lizhi Wang, et al. Adaptive nonlocal sparse representation for dual-camera compressive hyperspectral imaging. IEEE Transactions on Pattern Analysis and Machine Intelligence, 2016, 39(10): 2104-2111.
[5] Ying Fu, et al. Exploiting spectral-spatial correlation for coded hyperspectral image restoration. IEEE Conference on Computer Vision and Pattern Recognition. 2016: 3727-3736.
[6] Zhiwei Xiong, et al. Hscnn: Cnn-based hyperspectral image recovery from spectrally undersampled projections. IEEE International Conference on Computer Vision Workshops. 2017: 518-525.
[7] Choi I, et al. High-quality hyperspectral reconstruction using a spectral prior. ACM Transactions on Graphics, 2017, 36(6):218.
[8] Lizhi Wang, et al. Hyperreconnet: Joint coded aperture optimization and image reconstruction for compressive hyperspectral imaging. IEEE Transactions on Image Processing, 2018, 28(5): 2257-2270.
[9] Jian Zhang, Ghanem B. ISTA-Net: Interpretable optimization-inspired deep network for image compressive sensing. IEEE Conference on Computer Vision and Pattern Recognition. 2018: 1828-1837.
[10] Lizhi Wang, et al. Hyperspectral image reconstruction using a deep spatial-spectral prior. IEEE Conference on Computer Vision and Pattern Recognition. 2019: 8032-8041.

Thanks for your attention!